Modelling and Computer Simulation of Aerodynamic Interactions in High-Rise Lift Systems

S. Mirhadizadeh[1], S. Kaczmarczyk[1], N. Tongue[1], H. Al-Jelawy[1]
P. Feldhusen[2], W Delk[2], K. Anderson[2], F. Dudde[2]

[1]School of Science and Technology, The University of Northampton, UK
[2]ThyssenKrupp Elevator AMS, Research and Innovation Center Horn Lake, USA

Keywords: High-Speed Lifts, Multibody Dynamics, Computational Fluid Dynamics, Computer Simulation.

Abstract. The aerodynamic effects that occur when a high-speed lift travels through the hoistway involve a range of diverse phenomena that lead to excessive vibrations of the sling-car assembly and noise inside the hoistway and the car. Noise and vibration may then be transmitted to the building structure. Thus, a good understanding and prediction of aerodynamic phenomena occurring in high-speed lift installations is essential to design a system which satisfies ever more demanding ride quality criteria. This paper discusses the fluid-structure interactions taking place in high-rise applications and presents the results of a study to develop a computational model to predict the aerodynamic interactions in high-speed lift systems using Multibody Dynamics (MBD) and Computational Fluid Dynamics (CFD) techniques. The model is implemented in a high-performance computer simulation and 3D visualisation platform. It is demonstrated that the model can be deployed as a tool for aerodynamic design and optimization of high-rise lift systems.

1 INTRODUCTION

The operation of lift systems is affected by vibrations and associated vibro-acoustic noise. This affects ride quality and results in a high level of dynamic stresses in elevator components.

The underlying causes of vibration in a lift system are varied, including poorly aligned guide rail joints, eccentric pulleys and sheaves, systematic resonance in the electronic control system, and gear and motor generated vibrations [1]. In high-rise applications lifts are subject to extreme loading conditions. High-rise buildings sway at low frequencies and large amplitudes due to adverse wind conditions and the load resulting from the building sway excites the elevator system. This results in large vibratory motions of elevator ropes. The taller a building, the higher the rated speeds of elevator systems are needed. The vibrations are increased as the speed increases. Torque ripple generated in the motor causes vertical vibrations of the car. At high speeds guide rail deformations induce large lateral vibrations of the car. Furthermore large aerodynamic loadings due to the airflow around the car result in excessive noise and flow-induced vibrations of the car structure.

A good understanding and prediction of vibration phenomena occurring in lift installations is essential for developing vibration suppression and control strategies in order to design a system which satisfies ever more demanding ride quality criteria. Therefore it is of benefit to apply computer simulation techniques to address vibration problems in high-speed high-rise lift (HRHSL) systems.

2 MULTIBODY SYSTEM AND FLUID-STRUCTURE INTERCATIONS MODEL

Vibration sources affecting the dynamic behaviour of a car in a HRHSL system include the excitations applied due to air flow interactions (FSI), imperfections of the guiding systems and the influence of dynamics of suspension and compensating ropes (MBD), see Figure 1.

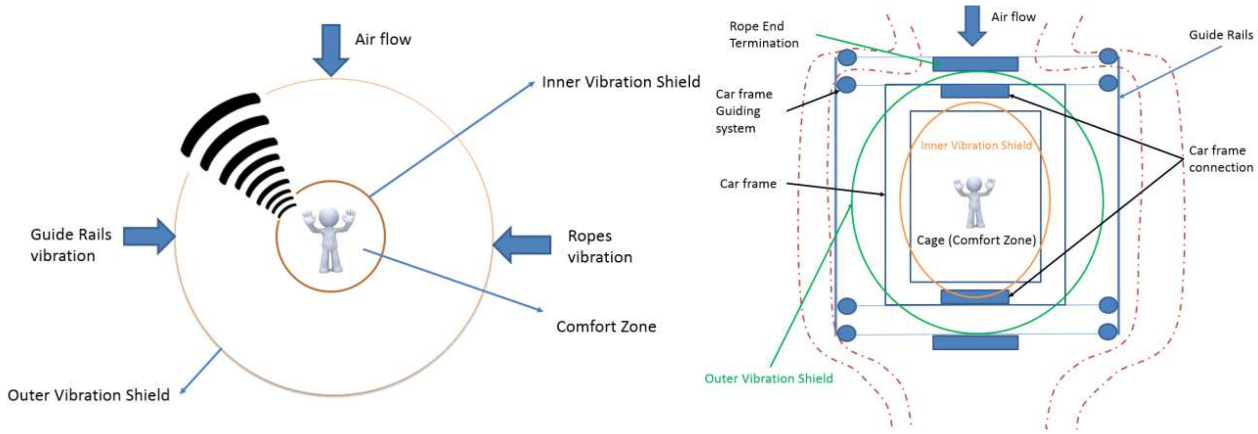

Figure 1 Vibration and Noise Excitation Sources

2.1 Air flow-induced vibrations and noise

The aerodynamic phenomena affect the performance of HRHSLs. At high speeds the air flow around the car – frame assembly induces excessive vibrations and noise. During the lift travel large air pressure differences between the front and rear of the car are being generated [2]. Furthermore, the effects due to multiple cars running in the same shaft cannot be neglected. Funai et al. [3] conducted a computer simulation case study into these effects when two cars run parallel to and pass each other in a hoistway. The results indicate that the dominant frequency of air pressure fluctuations in the former case is around 3.7 Hz being close to the out-of-phase mode of the car – frame vibration mode. On the other hand, the dominant frequency of air pressure fluctuations in the latter case was 2.2 Hz.

A study to characterize the most important vibro-acoustic energy sources and identify the dominant paths of broadband (100 – 500 Hz) acoustic energy transmission to the car interior in HRHSL installations has been carried out by Coffen et al. [4]. It has been identified that lift cars are subject to structure-borne as well as to air-borne noise. Structure-borne noise is caused mainly by the vibration induced by the car roller guides – guide rail interaction and by the hoist rope – rope hitch interface. This structure-borne vibro-acoustic energy is transmitted to the car interior through the car frame structure (and in particular by the uprights).

The air-borne noise is generated by aerodynamic effects during the car travel. It includes shaft noise entering the car through the ventilation openings and the door seals. The wind (flow)-induced vibrations of the car exterior panels generate noise that is transmitted to the car interior.

Finite element modelling, modal analysis and statistical energy analysis (SEA) are used as noise prediction techniques. The latter technique have yielded accurate results and facilitated the identification of the dominant sources and paths of vibro-acoustic energy in the lift car assembly [4]. Namely, it has been concluded that at higher speeds (over 9 m/s) the dominant path was air-borne noise radiating through the acoustic leaks and non-resonant energy transmission. The secondary path was identified as structure-borne noise arising from the car floor. However, at lower velocities (5 m/s) the contributions to interior car noise were the same for both paths.

2.2 Modelling Methodology

A HRHSL installation can be considered as a multi-body system (MBS) with discrete and continuous (distributed-parameter) components. The diagram presented in Figure 2 illustrates the modelling process of the MBS. The components of known geometry, mass, stiffness and damping characteristics are subjected to constraints applied at their boundaries and their responses exhibit non-stationary, nonlinear coupled modes of motion.

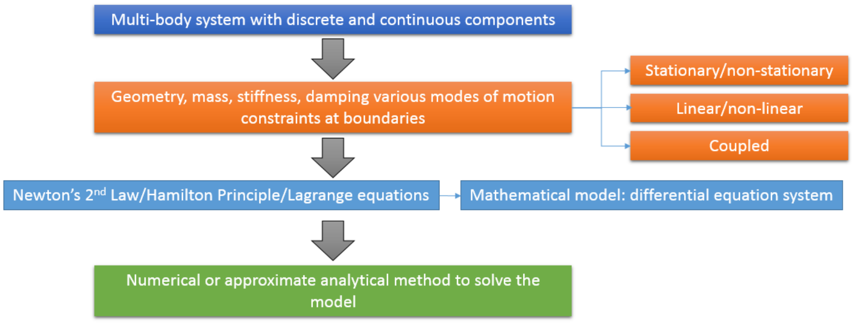

Figure 2 MBS modelling process.

In order to derive the differential equations of motion (the mathematical model) of such a system Newton's 2nd law or Hamilton principle/ Lagrange's Equations techniques can be applied [5]. The use of Hamilton principle/ Lagrange equations facilitates the derivation of equations of motion in terms of generalized coordinates, without the need of free body diagrams. The structure model can then be stated as

$$\frac{d}{dt}\left(\frac{\partial T}{\partial \dot{q}_i}\right)-\frac{\partial T}{\partial q_i}+\frac{\partial V}{\partial q_i}+\frac{\partial \Re}{\partial \dot{q}_i}=Q_i^{nc}, \quad i=1,2,\ldots,n \tag{1}$$

where q_i is the generalized coordinate, $\dot{q}_i=\partial q_i/\partial t$ represent the generalized velocity, $T(\mathbf{q},\dot{\mathbf{q}})$ is the total kinetic energy of the system, $V(\mathbf{q})$ is the total potential energy of the system, $\Re(\dot{\mathbf{q}})$ denotes Rayleigh dissipation function and Q_i^{nc} is the non-conservative generalized force corresponding to the generalized coordinate q_i.

In general, the equations of motion (1) are of a non-stationary and nonlinear nature and their closed-form analytical solutions are not available. But they can be treated by approximate analytical methods (such as perturbation analysis). However, the most convenient approach is to use direct numerical integration (numerical simulation) techniques.

The fluid model is expressed in terms of Navier–Stokes (N-S) equations that represent the conservation of momentum formulated as

$$\rho\left(\frac{\partial \mathbf{V}}{\partial t}+\mathbf{V}\cdot\nabla\mathbf{V}\right)=-\nabla p+\rho\mathbf{g}+\mu\nabla^2\mathbf{V}+\mathbf{F} \tag{2}$$

where $\mathbf{V}$ is the fluid velocity, $\mathbf{p}$ is the fluid pressure, ρ denotes the fluid density, μ is the fluid dynamic viscosity and $\mathbf{F}$ represents external foces applied to the fluid.

The N-S equations are solved together with the continuity equation representing the conservation of mass given as

$$\frac{\partial \rho}{\partial t}+\nabla\cdot(\rho\mathbf{V})=0 \tag{3}$$

3 COMPUTER SIMULATION TESTS AND RESULTS

The fluid flow is coupled to the structure and the solution scheme is based on Lagrangian formulation for the structure and Arbitrary Lagrangian-Eulerian (ALE) formulation [6] for the fluid regions.

A 3D CAD assembly model of an elevator courtesy of Thyssenkrupp Elevator has been used, see Figure 3, to combine the finite element (FE) analysis on the shroud structure, multibody dynamics (MBD) and computational fluid dynamics (CFD) of the car-sling system.

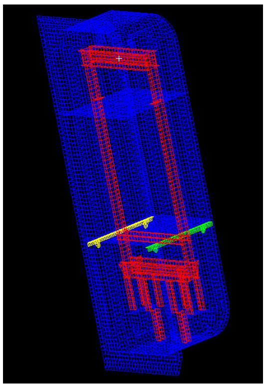

MBD of the car-sling system

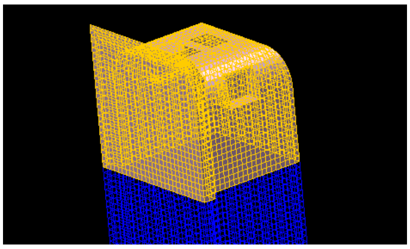

FE analysis on the shroud

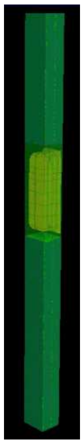

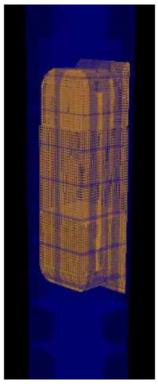

CFD Elevator Shaft

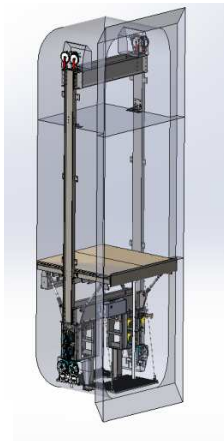

Figure 3 3D CAD assembly model of an elevator courtesy of Thyssenkrupp Elevator

This study was conducted using the base model (in 3D) with an elevator car of mass P = 1000 kg (including the shroud) which is supported by a platform mounted within a sling on elastomeric isolation pads of combined stiffness coefficient k_p = 29 kN/m. The car frame mass is M = 400 kg and the car – frame assembly is suspended on 4 steel wire ropes in 1:1 configuration. The ropes are of modulus of elasticity E = 0.85 × 105 N/mm2, mass per unit length m_r = 0.66 kg/m, metallic (effective) area A_{eff} = 69 mm2 (see Table 1). The car is traveling in the hoistway of dimensions 2.5m x 3m (used for creating a meshed shaft model) over the time interval of 30.2 seconds (the materials for car and shroud have been assumed as steel and isotropic aluminum, respectively) with the car travelling at the maximum speed of 10 m/s.

Table 1 Fundamental parameters of the system

Parameter	Value	Unit
Car	1000	kg
Frame	400	kg
m_r	0.66	kg/m
E	85000	N/mm^2
A_{eff}	69	mm^2
Stiffness of cable spring	7.82	kN/m
Stiffness of spring	29	kN/m
Damping coefficient	20	kNs/m

The air properties are considers as density of 1.14 kg/m3, specific heat ratio of 1.401 at 20 0C with gas constant (R) of 287 J/ (kg.K). The coupling has been considered only for shaft, top/bottom shroud and around car as a velocity, pressure and density parameters with both side flow (in and out).

The computer simulation tests are executed in Dytran [7]. Dytran involves a fluid solver based on the Finite Volume Method (FVM) in which Eulerian mesh is used, as well as a structure solver based on the Finite Element Method (FEM) in which Lagrangian mesh is used. Two interactions could be applied by using Dytran, structure-structure interaction which is based on contact algorithms, and fluid-structure interaction which is based on coupling algorithms. This software has been used to analyse the complex non-linear behaviour of lift structures interacting with air/fluid-flow. Eulerian and Lagrangian meshes can be utilized in the same analysis as well as coupled together allowing the solution of FSI problems (MSC. software Corporation, 2013).

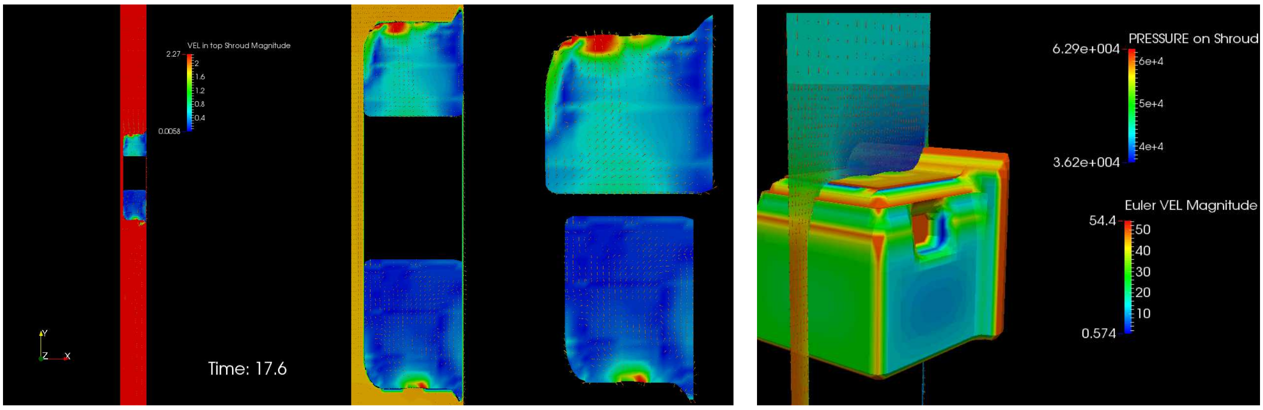

Figure 4 **Air flow velocity and pressure profile around the shroud and around the car**

Figure 4 shows that the velocity magnitued at the the inside of the shroud can reach the maximum of 2.27m/s, with the car travelling at the constant speed of 10 m/s the pressure acting upon the shroud, with its maximum of 62.9 kPa, together with the velocity profile around the top part of the shroud, the maximum is 54.4 m/s. With same scale factor there are areas at the bottom of the shroud that reach the same maximum velocity.

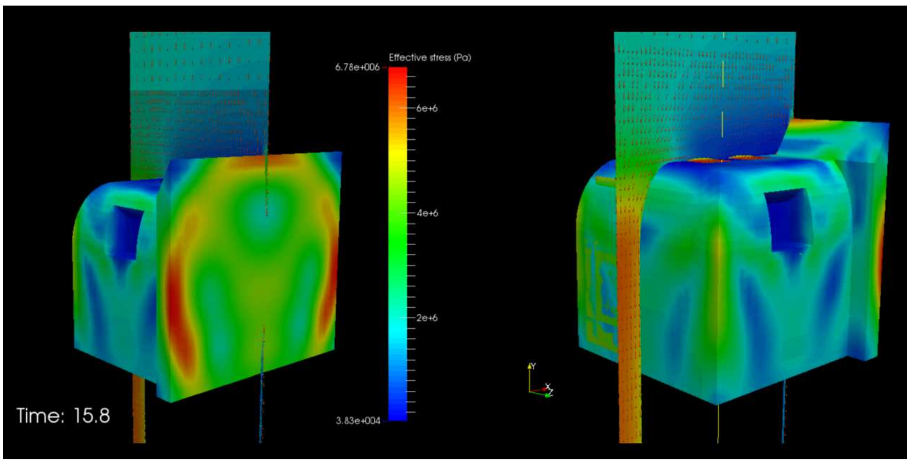

Figure 5 **Effective stress in the shroud**

Figure 5 is representing the effective stress (EFFST) defined by equation (2), showing the effective stress on the shroud which can reach 6.78 MPa, for the front and back of top shroud, respectively, where σ_x, σ_y and σ_z denote the normal stress components and τ_{xy}, τ_{yz} and τ_{zx} are the shear stress components in the X, Y and Z directions, respectively.

$$\bar{\sigma} = \sqrt{\tfrac{1}{2}\left[\left(\sigma_x - \sigma_y\right)^2 + \left(\sigma_y - \sigma_z\right)^2 + (\sigma_z - \sigma_x)^2\right] + 3(\tau_{xy}^2 + \tau_{yz}^2 + \tau_{zx}^2)} \tag{2}$$

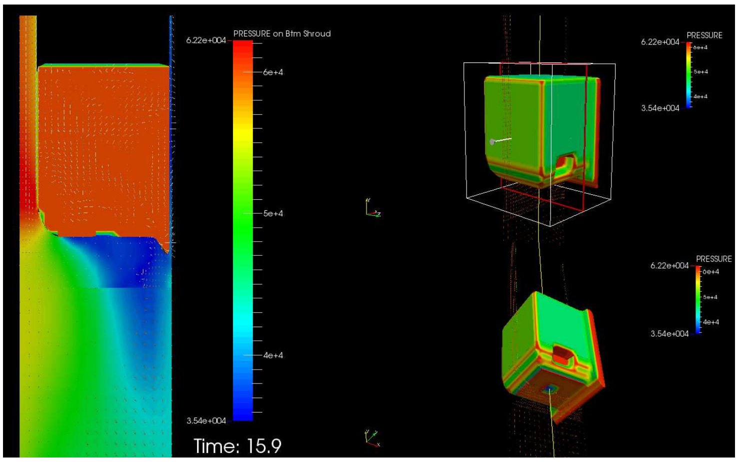

Figure 6 Pressure effect around car and inside of bottom shroud

Figures 6 show the pressure distribution at the bottom part of the shroud with the maximum value of 62.9 kPa, together with the velocity profile which can reach 2.27 m/s.

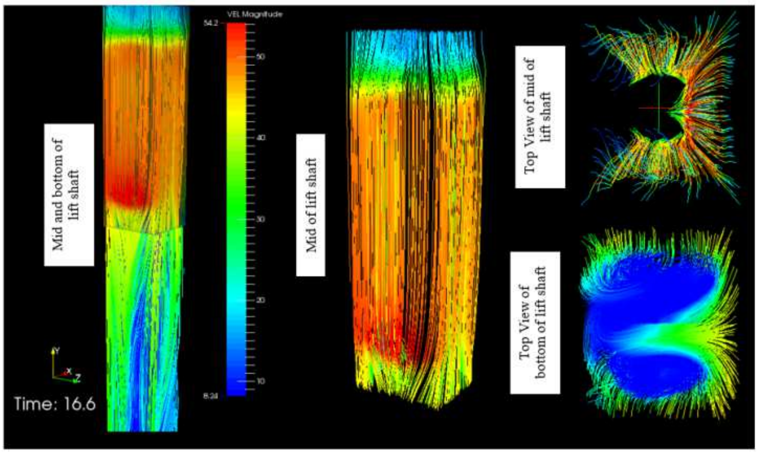

Figure 7 Velocity streamline profile in the elevator shaft

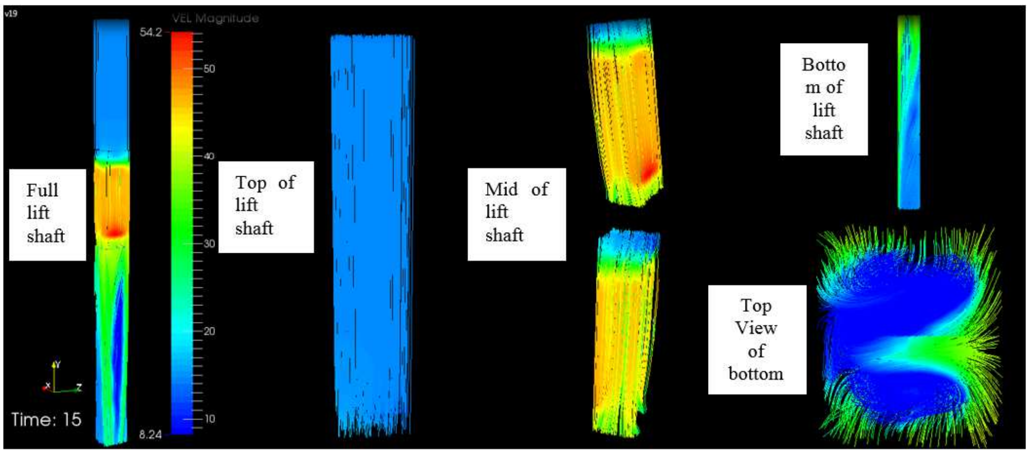

Figure 8 Velocity streamline profile in the elevator shaft

Figures 7 and 8, present Streamlines, which are instantaneously tangent to the velocity vector of the flow for the mid and bottom of the elevator shaft.

4 CONCLUSIONS

This research describes the use of integrated multidisciplinary analysis for modelling and simulation of the dynamic interactions in high-speed elevator systems using a high-performance computer simulation platform. An explicit nonlinear Computational Fluid Dynamics (CFD) solution is used to predict the fluid-structure interactions (FSI). The CFD solution is combined with Multibody Dynamics (MBD) simulation and Finite Element (FE) analysis to determine the dynamic responses and resulting loads due to the complex FSI arising in the system. As a result, this research developed a computer simulation software platform combining the MBD, FE and CFD techniques for the prediction of vibration responses arising in high-speed high-rise elevator (HRHSE) systems.

Further work would be required to optimize further the software platform and hardware configuration in order to reduce simulation time, to test the model performance and to fully integrate all possible excitation sources into the models. Experimental tests should then be carried out to validate the model and simulation results in the next stage.

REFERENCES

[1] J.P. Andrew, and S. Kaczmarczyk, Systems Engineering of Elevators. Elevator World, Inc., Mobile, Alabama, 2011.

[2] G.X. Shen, H.L. Bai, A.T.P. So, Experiments on Aerodynamics of Super High Speed Elevators. Elevator Technology 15, Proceedings of ELEVCON 2005, June 2005, Beijing, China, pp. 174–184.

[3] K. Funai, H. Katayama, J-I. Higaki, K. Utsonomiya, S. Nakashima, The Development of Active Vibration Damper for Super High-Speed Elevators. Elevator Technology 14, Proceedings of ELEVCON 2004, April 2004, Istanbul, Turkey, pp. 81-89.

[4] C. Coffen, L. Hardin, T. Derwinski, Statistical Energy Analysis of a High Speed Elevator Cab and Frame. Proceedings of the 5th International Congress on Sound and Vibration, December 15-18, 1997, Adelaide, South Australia.

[5] S. Kaczmarczyk, Prediction and analysis of the dynamic behaviour and vibrations of lift systems. European Lift Congress 2014. Technical Academy of Heilbronn eV, Stuttgart 7-8 October 2014.

[6] Y. Bazilevs, K. Takizawa, T.E. Tezduyar, Computational Fluid-Structure Interaction: Methods and Applications. Wiley & Sons Ltd, Chichester, United Kingdom, 2013.

[7] MSC Software Corporation, Dytran Explicit Solution for Transient Structural Dynamics and Fluid-Structure Interaction. Product Datasheet – Dytran™.